LIMNOLOGY and OCEANOGRAPHY

ASLO

Limnol. Oceanogr. 9999, 2021, 1–14

doi: 10.1002/lno.12004

Dissolved organic carbon as a driver of seasonal and multiyear phytoplankton assembly oscillations in a subtropical monomictic lake

Kristy Lee Sullivan [1]*, **Evelyn E. Gaiser** [1], **Hilary M. Swain** [2]

[1]Department of Biological Sciences and Institute of Environment, Florida International University, Miami, Florida
[2]Archbold Biological Station, Venus, Florida

Abstract

Phytoplankton assembly dynamics in lakes are highly sensitive to variability in climate drivers and resulting physicochemical changes in lake water columns. As climate change increases the frequency of major precipitation events and droughts, many lakes experience increased inputs of colored dissolved organic carbon (CDOC) and nutrients. How these CDOC-related changes in resources, transparency, and thermal stability affect phytoplankton assemblages, succession, and resilience is understudied, particularly in subtropical lakes. Here, we used time series, multivariate, and trait-based functional redundancy analyses to elucidate the roles of phytoplankton in ecosystem resilience and determine potential drivers of assemblage shifts in a subtropical monomictic lake with fluctuating CDOC inputs (Lake Annie, Highlands County, Florida, USA). We found that phytoplankton assemblages and successional patterns differed between two dark-water states (late 2005–mid-2007, late 2012–2019) bracketing a clear-water state (mid-2007–late 2012), caused by shifting CDOC and nutrient concentrations associated with oscillating groundwater levels. Diatoms (Bacillariophyta), which were dominant during the two dark-water states, nearly disappeared and were replaced by synurophytes during the clear-water state. Assemblages had greater interannual consistency in the dark-water states, while mean functional redundancy decreased in the clear-water state. Seasonal phytoplankton successional changes were also more pronounced and synchronized with seasonal hydrologic shifts in the dark-water states. Multiyear assemblage shifts occurred more quickly in clear-to-dark than dark-to-clear state transitions, suggesting phytoplankton in dark-water states may be more resistant to state transitions or even contribute to dark-water state resilience via feedback loops.

Climate and land use change are altering the supply of dissolved organic carbon (DOC) and nutrients to lake ecosystems at regional and global scales (Pace and Cole 2002). Concomitant reductions in water transparency, acidification, and suppression of bacterial and primary productivity caused by increased colored DOC (CDOC) inputs have led to transitions of lakes across the trophic spectrum to brown-water states (Carpenter and Pace 1997; Solomon et al. 2015; Kritzberg et al. 2020). The effects of these transitions on lake biota as well as their reversibility are poorly understood due to a lack of long-term studies and few instances of naturally occurring state reversions (Pace and Cole 2002; Bergström and Karlson 2019). Determining how phytoplankton assemblages respond to long-term changes in CDOC input on seasonal to interannual timescales will illuminate the consequences of CDOC shifts on phytoplankton dynamics and whether lakes can be resilient to water color shifts.

An ecosystem's ability to maintain its existing state is founded on resilience, or the amount of internal and external perturbations a system can withstand before shifting to an alternative state (Holling 1973; Angeler and Allen 2016). In browning lakes, the suppression of bacterial activity by refractory CDOC is a pertinent example of a feedback that increases resistance to state change (Carpenter and Pace 1997; Standish et al. 2014). Furthermore, the quality of allochthonous DOC can affect autochthonous DOC production, also influencing resilience (Kelly et al. 2018; Olson et al. 2020). Widespread lake browning and interactions with phytoplankton assemblages are of recent interest in limnology (Deininger et al. 2017; Wilken et al. 2017; Senar et al. 2021), yet knowledge of the reversibility of these conditions and specific phytoplankton assemblage responses or contributions to recovery are less well documented.

*Correspondence: ksull027@fiu.edu

Additional Supporting Information may be found in the online version of this article.

Special issue: Nonlinear dynamics, resilience, and regime shifts in aquatic communities and ecosystems.

Browning may occur in pulses as a result of intense or even moderate rainfall events, the frequency of which are expected to increase with a warming climate (Pendergrass et al. 2017; Kritzberg et al. 2020; Stockwell et al. 2020). Large pulses of mineralized allochthonous organic matter and nutrient runoff are most often delivered to lakes following periods of flooding or continuous water table saturation when accumulation of organic matter is faster than mineralization rates in the watershed (Gaiser et al. 2009a; Solomon et al. 2015). As most allochthonous DOC is highly colored (Bertilsson and Tranvik 2000), lakes may be particularly subject to browning when exposed to alternating wet–dry periods due to oscillations in rainfall. Climate teleconnections such as the El Niño Southern Oscillation (ENSO), Pacific Decadal Oscillation (PDO), or Atlantic Multidecadal Oscillation (AMO) are associated with rainfall oscillations, driving physical and biological shifts in lakes over interannual to multidecadal timescales (Harris and Baxter 1996; Winder and Schindler 2004; Gaiser et al. 2009b). Because large influxes of allochthonous DOC tend to dissipate slowly from lakes due to their highly refractory nature, extended periods of brown water may occur despite subsequent natural or managed decreases in allochthonous inputs (Carpenter and Pace 1997; Solomon et al. 2015). Long-term data from lakes with oscillating inputs of CDOC provide an opportunity to examine the resilience of brown- and clear-water states.

Light limitation caused by browning can lead to increased numbers of mixotrophic phytoplankton such as cryptomonad *Cryptomonas*, and ochrophytes *Dinobryon* and *Gonyostomum semen* (Wilken et al. 2017; Kritzberg et al. 2020). Because mixotrophs are capable of both autotrophy and heterotrophy, they may persist and outcompete other taxa even if allochthonous DOC inputs decline (Jones 2001; Wilken et al. 2017). The presence of mixotrophic taxa may also increase the functional redundancy (the number of different species/taxa filling similar functional roles, Angeler and Allen 2016, Ricotta et al. 2016) of a phytoplankton assemblage, due to their diverse functional forms (Leles et al. 2018). General ecological theory suggests when functional redundancy is high, the loss of a given species is less likely to have a strong effect on ecosystem function, making functional redundancy a suitable proxy for resilience (Standish et al. 2014; Ricotta et al. 2016). Examining the relationship between phytoplankton assembly and environmental change using functional group or trait-based approaches can also improve understanding and prediction of community change and may provide additional indication of resilience in lake ecosystems (Reynolds et al. 2002; Kruk et al. 2010, 2017).

Subtropical monomictic Lake Annie (Highlands County, Florida, USA) is a meso-oligotrophic lake with oscillating CDOC inputs revealed by water clarity and physicochemical data collected over 30+ yr (Gaiser et al. 2009a) that are correlated with the AMO (Gaiser et al. 2009b). Water table height increases during the warm (positive) phase of the AMO causing increased surface and groundwater inflows to Lake Annie, which increase lake water stage and concentrations of allochthonous CDOC (Gaiser et al. 2009a,b). In contrast, the cold (negative) AMO phase reduces precipitation intensity, variability, and amount in Central Florida (Enfield et al. 2001; Curtis 2008), reducing groundwater levels and surface water flows to the lake. With lessened allochthonous CDOC input, water clarity tends to increase in these years, as observed historically from 1962 to 1993 (Battoe 1987; Gaiser et al. 2009a). Although AMO phases occur in 65–80 yr intervals, precipitation patterns in Florida are also influenced by shorter timescale teleconnections such as the PDO, ENSO, and their interactions with regional climate variability (Enfield et al. 2001; Moses et al. 2013).

Given the strong multiyear oscillatory CDOC pattern in Lake Annie, we expected to observe a difference in phytoplankton assemblages between periods of dark- and clear-water color states, driven by the effects of CDOC delivery on light, nutrients, and thermal stability (H1, Fig. 1). During dark-water states, we predicted increased ecosystem resilience, measured by interannually consistent phytoplankton assemblages with greater mean functional redundancy (H1a). During the clear-water state, we predicted reduced resilience, measured by interannually inconsistent phytoplankton assemblages with lower mean functional redundancy (H1b). We hypothesized a stronger relationship between phytoplankton assemblage and external (hydrologic) controls during dark-water states due to increased groundwater stage (H2). This difference could be driven by changes in abiotic and biotic regulation where dark-water assemblages may be maintained by external drivers (CDOC, nutrients) and biological feedback loops, while clear-water assemblages may be more strongly influenced by biological interactions alone. Here, we use time

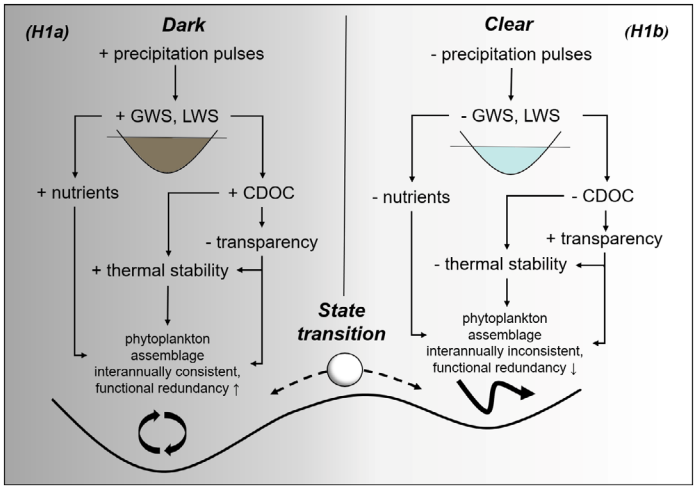

Fig. 1. Conceptual diagram of anticipated drivers of phytoplankton succession in dark-water (H1a, left) and clear-water (H1b, right) states based on the theoretical ball-and-cup model of system stability. Abbreviations GWS and LWS are defined as ground water stage and lake water stage, respectively.

series and multivariate analyses alongside a trait-based functional redundancy analysis to elucidate the potential drivers of phytoplankton assemblage shifts and roles of phytoplankton in lake ecosystem resilience to fluctuating CDOC inputs.

Materials and methods

Study site

Lake Annie is a small (0.364 km^2) yet deep (Z_{max} = 21 m) meso-oligotrophic lake located in Highlands County, Florida, USA (27°12′35″N, 81°20′57″W). The lake lies within the protected watershed of Archbold Biological Station (Archbold) 33.7 m above mean sea level (amsl) on 60–80 m of sand and clay sediment (Bishop 1956).

Physicochemical sampling and analysis

Monthly limnological sampling began in 1983 with the addition of phytoplankton sampling in late 2005. Data were collected monthly from the water column in 1 m intervals at the deepest point of the lake (20.7 m), including measurements of pH with a YSI Pro Plus handheld meter, and dissolved oxygen (DO) and temperature using a YSI Model 58 portable meter (2005–2010) and YSI Pro20 (2010–present). Thermocline depth and Schmidt stability were calculated from temperature profiles in RStudio v. 1.2.5001 (R Core Team 2019) using the *rLakeAnalyzer* package (Winslow et al. 2019). Oxycline depth was determined as the depth where DO < 0.5 mg L^{-1}.

Total monthly precipitation was measured at Archbold's National Weather Service Cooperative Main Grounds Weather Station. Monthly mean lake water stage and water residence time were calculated from a georeferenced stage recorder installed near the northern outlet of the lake. Mean groundwater stage was calculated from weekly measurements of a well upslope from the lake at 63.7 m amsl. Teleconnection index values for the AMO, PDO, and Southern Oscillation Index (SOI) were obtained from the National Oceanic and Atmospheric Administration National Centers for Environmental Information website.

Light extinction rate (K_d m^{-1}) was calculated from photosynthetically active radiation (PAR) measured at 1-m intervals using a LiCor LI 188B Integrating Photometer with 2 pi surface and underwater sensors (2005–2015) and a LiCor LI 1500 (2016–present) coupled with Secchi disc values to evaluate the light environment (Gaiser et al. 2009a,b). Surface water samples were analyzed monthly for chlorophyll *a* (Chl *a*), total phosphorus (TP), and total nitrogen (TN) by spectrophotometry. Water color was measured monthly using the platinum-cobalt scale method for 2010–2015 and limited to quarterly thereafter given the strong relationship to DOC (r = 0.91, Florida LAKEWATCH 2020). Monthly surface water samples for TOC and DOC were stored in the dark at 4°C until analysis at Florida International University. After acidifying to pH < 2, and purging with CO_2-free air, TOC was measured by direct injection onto a hot platinum catalyst in a Shimadzu TOC-5000 analyzer. The same method was used to measure DOC after filtration through a 0.45-μm ashed filter.

Phytoplankton sampling, identification, and enumeration

Phytoplankton were collected using 10 m vertical tows of a 20-μm net, preserved with 1% glutaraldehyde and refrigerated until analysis. A subsample of concentrated phytoplankton was mounted onto a semi-permanent slide and enumerated for relative phytoplankton abundance using either a Zeiss Axioskop 2 microscope at ×640 magnification or a Nikon Eclipse E600 microscope at ×600 magnification. At least 500 natural units (individual cells, colonies, or filaments) were counted and identified to the lowest possible taxonomic level.

Research design

Because not all DOC is colored (Bertilsson and Tranvik 2000), water color as PCUs was chosen as the metric of water color state. Canfield et al. (1984) previously classified Florida lakes as visibly colored (dark) during periods when water color was greater than 20 PCUs; however, 30 PCUs was used as the cutoff in this study as water color was consistently below this threshold for an extended period of time. For all variable analyses, the time series was broken into three states defined by shifts in water color above or below a threshold of 30 PCUs (Fig. 2). Groupings include states *dark-water 1* (October 2005–October 2007), *clear-water* (November 2007–September 2012), and *dark-water 2* (October 2012–December 2019). Because water color was only measured quarterly for a large portion of this study, missing monthly data (48% of values) were interpolated by averaging the prior and subsequent values to form a continuous time series. The time series was decomposed using moving averages with a multiplicative model to examine the long-term movement of water color (trend component) by eliminating noise and seasonal components of the data set. A Chow test for a structural break was used to determine significant differences between dark- and clear-water states using base R statistical functions in RStudio v. 1.2.5001 (Chow 1960; R Core Team 2019). Dark-water 1 and the clear-water state demonstrate a structural break (Chow statistic = 193.73, F_{crit} = 1.69) as well as the clear-water and dark-water 2 state (Chow statistic = 59.55, F_{crit} = 1.50). These results were supported by Tukey HSD test results following a one-way ANOVA of the three states (dark-water 1, clear-water, and dark-water 2) for both water color and groundwater stage, calculated using PAST statistical software (Hammer et al. 2001).

Data analysis

Means (± SE) of 17 environmental variables were calculated for dark- and clear-water states including AMO Index, PDO index, SOI, precipitation as end of month total, monthly groundwater stage (m amsl), monthly lake water stage (m amsl), Secchi disk depth (m), PAR extinction rate as (K_d m^{-1}), TOC and DOC (mg L^{-1}), water color (PCUs), thermocline depth (m), Schmidt stability (J m^{-2}), oxycline depth (m), monthly mean pH, TP (μg L^{-1}), and TN (mg L^{-1}). Welch's

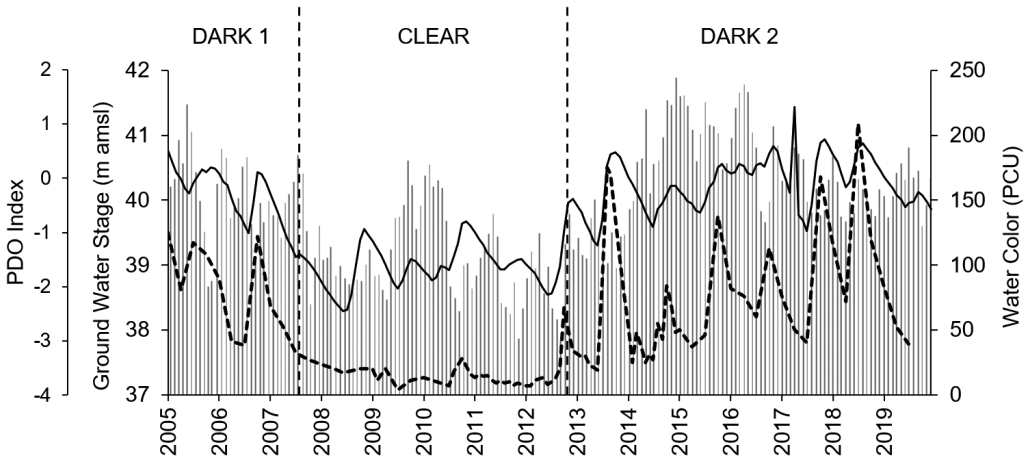

Fig. 2. Monthly mean groundwater stage (solid line), quarterly surface water color (dashed line), and monthly mean PDO index values (vertical gray bars). The first vertical line indicates a shift in surface water color < 30 PCU (dark-water state 1 to clear-water state) and the second vertical line indicates a shift in surface water color ≥ 30 PCU (clear-water state to dark-water state 2). Water color and groundwater stage were strongly correlated, $r = 0.79$.

t tests were used to determine differences ($*p < 0.05$) between states of unequal sample size using PAST statistical software (Hammer et al. 2001). The *t* scores were also reported as a measure of the size of the difference. Correlations between variables were calculated and visualized within a Pearson correlation matrix also using PAST (Hammer et al. 2001).

Missing phytoplankton samples for months April 2006, November 2006, January 2013, and June 2017 were excluded from all analyses except for time series analyses where values were interpolated using the means of the prior and subsequent month values. Taxon richness, Shannon diversity, taxon cell density (cells mL^{-1}) and taxon biovolume ($\mu m^3\ mL^{-1}$) were calculated for each sample. Taxon cell densities and biovolumes were converted to relative cell density and relative biovolume (% of total sample). Time series of these data were examined for each phylum. Each taxon was assigned to one of eight morphology-based functional groups (MBFGs). Following the outline of seven phytoplankton MBFGs proposed by Kruk et al. (2010), an eighth group was added to separate filamentous Charophyta and Chlorophyta from MBFG group 4. Groups include (1) small organisms with high surface area to volume ratio, (2) small flagellated organisms with siliceous exoskeletal structures, (3) large filaments with aerotopes, (4) medium size organisms lacking specialized traits, (5) medium to large size unicellular flagellates, (6) non-flagellated organisms with siliceous exoskeletons, (7) large mucilaginous colonies, and (8) large filaments lacking aerotopes (Supporting Information Table S1). Taxa undescribed by Kruk et al. (2010) but present in Lake Annie were assigned to the closest functional group based on their morphology. Temporal changes in mean percent contribution to biovolume of each functional group in the dark- and clear-water states were examined, and functional redundancy analyses were performed with functional unit data using methods outlined by Ricotta et al. (2016; *see* Supporting Information Methods). A Welch's *t* test and one-way ANOVA were used to determine differences ($*p < 0.05$) in functional redundancy between clear and dark states. Each taxon was also assigned a size class, small (0–100 μm^3), medium (101–1000 μm^3), or large (1001–300,000 μm^3), based on $\log_{10}$ transformed cellular biovolume.

Multivariate analyses including nonmetric multidimensional scaling (NMDS) ordinations were constructed using PRIMER-E v. 7.0.13 (Clarke and Gorley 2015) software to visualize dissimilarity among phytoplankton assemblages in dark- and clear-water states (*see* Supporting Information Methods). Following an initial cluster analysis, phytoplankton assemblage data were organized into three groups: *dark-phytoplankton assemblage 1* (October 2005–November 2009), *clear-phytoplankton assemblage* (December 2009–August 2013), and *dark-phytoplankton assemblage 2* (September 2013–December 2019) reflecting suspected response lags to water color state transitions. The initial two-dimensional NMDS ordination was rotated so that axis 1 was most strongly correlated with time (year). Axis 1 scores were examined as a decomposed time series in RStudio (R Core Team 2019) using moving averages with a multiplicative model. The time series was compared with the decomposed trend line of water color to visualize the lag time of assemblage change in response to water color shifts. A Chow test was used to test the significance of structural changes in the ordinations' axis 1 values regressed by time (Chow 1960; R Core Team 2019). A similarity percentage breakdown was used to calculate the contribution of each taxon to the dissimilarity between the three phytoplankton assemblage groups. Dark-phytoplankton assemblages 1 and 2 were then combined and compared with the clear-phytoplankton assemblage using the same analysis. Welch's *t* tests were performed using taxon richness, Shannon diversity,

and Chl *a* metrics as a univariate measure of difference (*$p < 0.05$) between dark- and clear-phytoplankton assemblages using PAST statistical software (Hammer et al. 2001). To observe trends over time, Bray–Curtis similarity matrix data were plotted as a scatter plot using months between samples as the independent variable. Two one-way analyses of similarity (ANOSIM) were also performed on the resemblance matrix data in PRIMER (Clarke and Gorley 2015). Samples were grouped by phytoplankton assemblage (dark 1, clear, and dark 2) and then by dark-phytoplankton assemblages combined and compared with clear-phytoplankton assemblages. Results were generated after 1000 permutations, and analyses had a significance level of 0.1%.

Results

Physicochemistry

Mean monthly groundwater stage was lower in clear-water than dark-water states and was positively correlated with water color ($r = 0.79$, Supporting Information Table S2). Water color did not differ between dark-water 1 and 2 states, and both dark periods had greater water color than in the clear-water state ($p < 0.001$). Unlike the longer period of record (1983–2009) where AMO was a significant driver of water color (Gaiser et al. 2009b), the correlation of AMO and SOI with water color during this period (2005–2019) was weaker ($r = 0.24$ and $r = -0.28$, respectively). The PDO was found to have a stronger correlation with groundwater stage ($r = 0.52$) and water color ($r = 0.35$). The dark-water states had a mean residence time of 9.1 months while the clear-water state had a mean residence time of 13.5 months.

Comparisons between dark-water and clear-water state monthly mean water color indicates strong seasonal trends in transparency during dark-water states (Table 1; Supporting Information Fig. S2). In contrast, the clear-water state monthly mean PAR extinction rate (K_d m^{-1}) shows decreased seasonality and variability. Mean extinction rate for a given dark-water state month was always greater than the corresponding clear-water state month, with September and October showing the greatest difference in extinction rates. Extinction rate was strongly correlated with groundwater stage ($r = 0.80$) and water color ($r = 0.92$, Supporting Information Table S2).

Of all 17 environmental variables (Supporting Information Table S3), 13 differed between dark-water 1 and 2 and clear-water state. Mean annual maximum groundwater stage and lake water stage were higher during the dark-water states (40.2 and 33.7 m amsl, respectively) and lower during the clear-water state (39.0 and 33.6 m amsl, respectively, Table 1), while there was no strong difference in summer thermocline depth and Schmidt stability between the two states (12.1 and 448.4 J m^{-2}, respectively, for dark-water state, 12.6 and 447.2 J m^{-2}, respectively, for clear-water state). Strong correlations ($r < -0.5$ or > 0.5) were found among all water clarity variables (Secchi depth, PAR extinction rate, TOC, DOC, and water color; Supporting Information Table S2).

Phytoplankton assemblage

A total of 279 taxa (morphologically distinct units) were identified from 8 algae phyla (Supporting Information Table S1) within the 167 monthly phytoplankton samples enumerated from October 2005 to December 2019. Although mean richness did not differ between dark- and clear-phytoplankton assemblages (30.1 ± 0.8 vs. 30.7 ± 1.2, respectively), Shannon diversity was different between assemblages (1.7 ± 0.1 vs. 2.0 ± 0.1, respectively). Chl *a* was higher in dark-phytoplankton assemblages than the clear-phytoplankton assemblage (4.7 ± 0.2 vs. 2.7 ± 0.2 $\mu g\ L^{-1}$, respectively). A lag

Table 1. Mean ± standard error (SE) of select physicochemical variables for the dark-water (PCU ≥ 30) and clear-water (PCU < 30) states. Dark-water states 1 and 2 (January 2005–October 2007 and October 2012–December 2019) were grouped for comparisons with the clear-water state (November 2007–September 2012). The *p* values (*$p < 0.05$) and *t* scores ($t_{crit} = 1.97$) for Welch's *t* test are presented in the last column. Variables include Pacific Decadal Oscillation (PDO) Index, precipitation as end of the month total (PPT), monthly mean groundwater stage (GWS), monthly mean lake water stage (LWS), thermocline depth, Secchi disk depth, surface water color (PCU), surface water total phosphorus (TP), and surface water total nitrogen (TN). For expanded table including all 17 physicochemical variables, see Supporting Information Table S3.

	Dark 1 and 2		Clear		Dark × Clear
Variable	**Mean ± SE**	***N***	**Mean ± SE**	***N***	***p* value (*t* score)**
PDO Index	−0.09 ± 0.08	121	−1.47 ± 0.10	59	< 0.001* (10.59)
PPT (cm)	10.67 ± 0.89	121	10.13 ± 1.19	59	0.717 (0.36)
GWS (m amsl)	40.17 ± 0.04	121	38.97 ± 0.04	59	< 0.001* (20.49)
LWS (m amsl)	33.71 ± 0.01	121	33.56 ± 0.01	59	< 0.001* (8.79)
Thermocline depth (m)	6.53 ± 0.27	121	7.93 ± 0.36	59	0.002* (3.10)
Secchi depth (m)	1.76 ± 0.06	121	4.05 ± 0.13	59	< 0.001* (15.79)
Water color (PCU)	71.33 ± 5.81	58	13.46 ± 0.95	35	< 0.001* (9.83)
TP ($\mu g\ L^{-1}$)	9.60 ± 0.33	121	5.66 ± 0.21	58	< 0.001* (10.07)
TN (mg L^{-1})	0.43 ± 0.01	121	0.29 ± 0.01	58	< 0.001* (9.30)

time of 25 months was detected between the dark-water 1 to clear-water state transition (November 2007) and the phytoplankton assemblage response (December 2009). A shorter lag time of 11 months was found between the clear-water to dark-water 2 state transition (October 2012) and the phytoplankton assemblage response (September 2013).

A large centric diatom, *Urosolenia* spp., was the most abundant diatom (Bacillariophyta) in the dark-phytoplankton assemblages contributing to 13.8% dissimilarity between the dark- and clear-phytoplankton assemblage groups (Supporting Information Table S1). Occasional increases of *Asterionella formosa* were also common during dark-phytoplankton assemblages. The largest change in assemblage structure throughout the study period was the near disappearance of diatoms in the clear-phytoplankton assemblage, synchronized with an increase in chrysophytes and synurophytes (Ochrophyta, Fig. 3). *Synura petersenii* and *Mallomonas* spp. dominated in the spring months in the clear-phytoplankton assemblage and together contributed to 7.1% of the dissimilarity between dark- and clear-phytoplankton assemblages (Supporting Information Table S1). Charophyta were abundant throughout the time series with *Staurodesmus triangularis* v. *inflatus* dominating both dark- and clear-phytoplankton assemblages. Charophyta relative abundance decreased during the clear-phytoplankton assemblage years, but relative biovolume increased, indicating the presence of larger species such as *Mougeotia* spp., *Staurastrum novae-caesareae*, and *Staurastrum ophiura*. Chlorophytes were also more abundant in the clear-phytoplankton assemblage, although relative biovolume remained consistent throughout the study period. Dinoflagellates (Miozoa) rarely contributed to more than 10% of relative abundance but due to their large size comprised a large portion of assemblage relative biovolume. *Fusiperidinium wisconsinense* and *Peredinium bipes* were the most common dinoflagellates during dark-phytoplankton assemblages, *F. wisconsinense* was also common during the clear-phytoplankton assemblage with *F. wisconsinsense* and *P. bipes* contributing to 5.4% and 5.2% of the dissimilarity between dark- and clear-phytoplankton assemblages, respectively (Supporting Information Table S1). Cyanobacteria relative abundance increased slightly during the clear-phytoplankton assemblage years, but relative biovolume remained low throughout the study period.

A 2D NMDS ordination with a minimal stress of 0.22 was achieved based on taxon relative biovolume (Fig. 4). Collective results of a one-way ANOSIM and NMDS ordination showed that clear- and dark-phytoplankton 2 assemblages were the most dissimilar (global *R*: 0.80), while dark-phytoplankton assemblages 1 and 2 were the most similar (global *R*: 0.31). Dark-phytoplankton assemblage 1 and the clear-phytoplankton assemblage were more similar but still distinct (global *R*: 0.45). A second one-way ANOSIM of the combined dark-phytoplankton assemblages with the clear-phytoplankton assemblage had a global *R* of 0.62. All ANOSIM values were significant. Water clarity and nutrients were the strongest drivers of phytoplankton assembly in the dark states with the Secchi depth vector showing the greatest influence ($r = -0.64$) aligned with axis 1 (Supporting Information Table S4). The precipitation vector was almost orthogonal to other hydrology and water clarity vectors, suggesting greater influence on axis 2. A Chow test of the relationship between axis 1 point values and time revealed a structural break between dark-phytoplankton assemblage 1 and the clear-phytoplankton assemblage (Chow statistic = 32.05, $F_{crit} = 1.69$) as well as between the clear- and dark-phytoplankton 2 assemblages (Chow statistic = 41.37, $F_{crit} = 1.63$).

Seasonal and interannual trends in phytoplankton sample similarity were observed in the Bray–Curtis phytoplankton assemblage resemblance matrix (Supporting Information Fig. S3). As expected in temporally autocorrelated data sets, similarity is highest among adjacent sample pairs, but was lowest around 6-yr interval pairs. There is a noticeable seasonal trend in the first segment of the graph among samples with 1–4-yr paired contrasts which dissipated toward the middle of the time series and reappears in 10–14-yr interval pairs, matching the dark- and clear-phytoplankton assemblage transition points. Seasonally, there was not a strong difference between assemblages (ANOSIM $R = 0.07$, nor a strong wet–dry seasonal difference between assemblages (ANOSIM $R = 0.04$); however, at least 5 dark years had 12-month return trajectories that were not evident in the clear years (Supporting Information Fig. S4).

The decomposed time series of NMDS axis 1 scores shows how the phytoplankton assemblage changes over time (Fig. 5). There is a strong decrease in axis 1 score values from 2010 to mid-2013 following a similar decrease in water color PCUs from mid-2007 to 2013. The previously determined lag time of around 25 months from initial PCU decrease below 30 units and phytoplankton assemblage shift was apparent, as well as the much shorter second lag between increase in PCU above 30 units and the second phytoplankton assemblage shift.

The phytoplankton assemblage data visualized by MBFGs reveals strong trends in phytoplankton functional group distribution between dark- and clear-phytoplankton assemblages (Fig. 6). While some functional groups were similarly distributed between assemblages (MBFGs 1, 3, and 7), other groups displayed greater relative abundance in dark-phytoplankton assemblages (MBFGs 4, 6, and 8), the clear-phytoplankton assemblage (MBFG 2) or a transitional assemblage (MBFG 5). Within the clear-phytoplankton assemblage, winter peaks of MBFG 2 were common, but absent in the dark-phytoplankton assemblages (Supporting Information Fig. S5). Mean functional redundancy was highest within the dark-phytoplankton assemblages, and the clear-assemblage demonstrated a lower and smaller range of functional redundancy values (Fig. 7). Combined dark-assemblage values were different from the clear-phytoplankton assemblage (Welch's *t* test, $p < 0.01$), though there was no significant difference between individual dark-assemblages (1 and 2) compared to the clear-assemblage

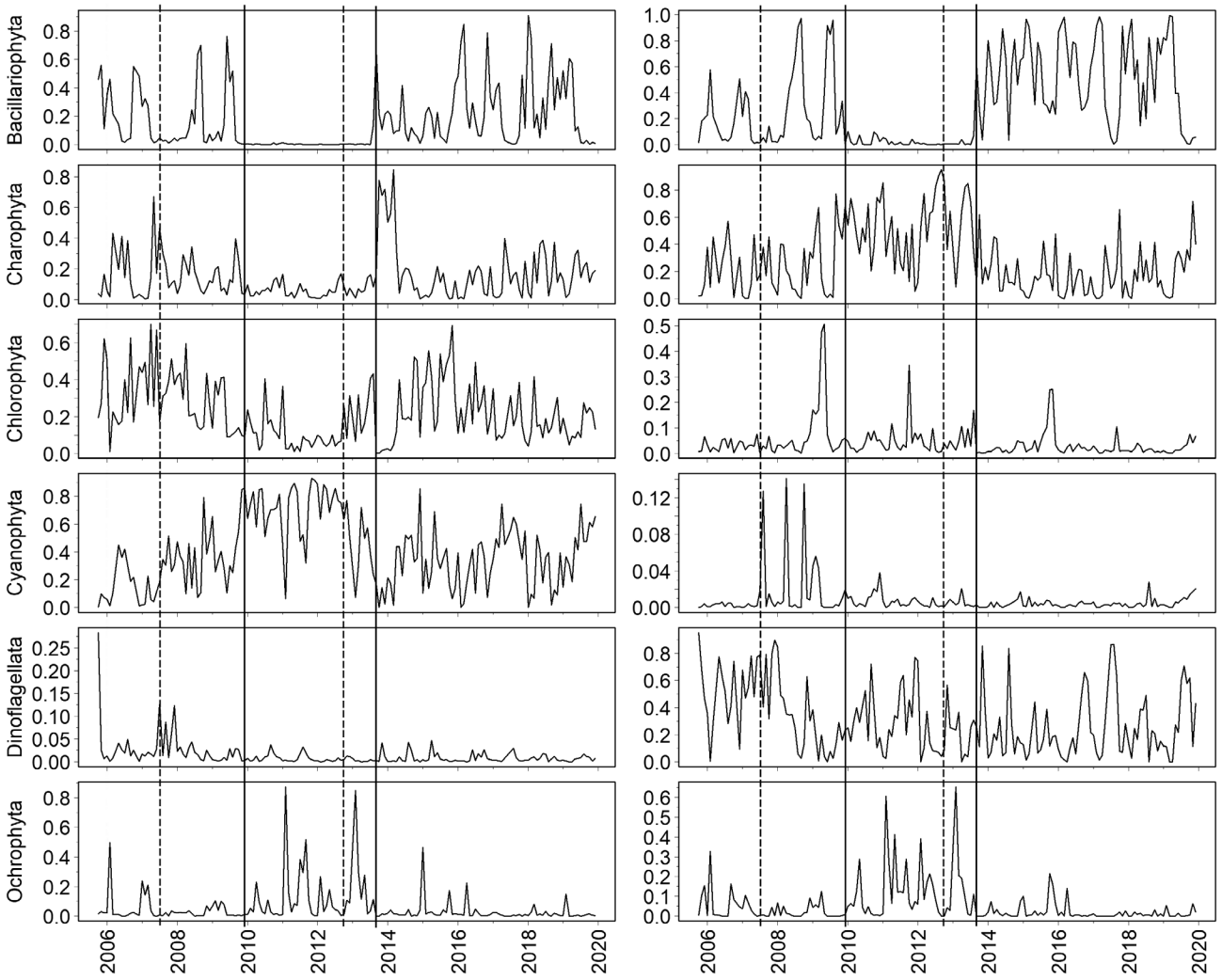

Fig. 3. Time series of phytoplankton relative cell density (left) and relative biovolume (right) of Bacillariophyta, Charophyta, Chlorophyta, Cyanophyta (Cyanobacteria), Dinoflagellata (Miozoa), and Ochrophyta (chrysophytes and synurophytes). Phyla Euglenophyta and Cryptophyta were excluded from this figure due to the low relative abundance and biomass of these taxa throughout the time series. Vertical dashed lines represent the clear- to dark-water state shift (see Fig. 2). The first vertical solid line indicates the delayed shift from dark- to clear-phytoplankton assemblages resulting from the initial water color state change, as determined by cluster analysis at a level of 22% similarity. The second vertical solid line indicates where the delayed shift from clear- to dark-phytoplankton assemblages occurred in response to the transition back to a dark-water state.

(one-way ANOVA, $p = 0.06$). Small taxa were found to contribute to a higher proportion of phytoplankton relative cell density in the clear-phytoplankton assemblage while large and medium taxa contributed to a higher proportion of phytoplankton relative cell density in dark-phytoplankton assemblages (Supporting Information Fig. S6).

Discussion

Phytoplankton composition, MBFGs, and seasonal dynamics differed among and within dark- and clear-phytoplankton assemblages, associated with interannual and seasonal fluctuations in water color and nutrients, supporting hypothesis H1. During dark-water states, seasonal phytoplankton successional changes were more pronounced and synchronized with seasonal hydrologic shifts (H1a), whereas during the clear-water state successional changes were dampened and mean functional redundancy decreased (H1b). However, because clear-state functional redundancy was not statistically distinct from individual dark states, our hypotheses of increased ecosystem resilience in dark states (H1a) and decreased ecosystem resilience in the clear state (H1b) are inconclusive. Multiyear shifts in MBFGs were associated with water color state shifts, with a stronger relationship between phytoplankton assemblage and external (hydrologic) controls in the dark states, supporting hypothesis H2. We expect the weakened connection between lake and watershed during the clear-water state reduced the

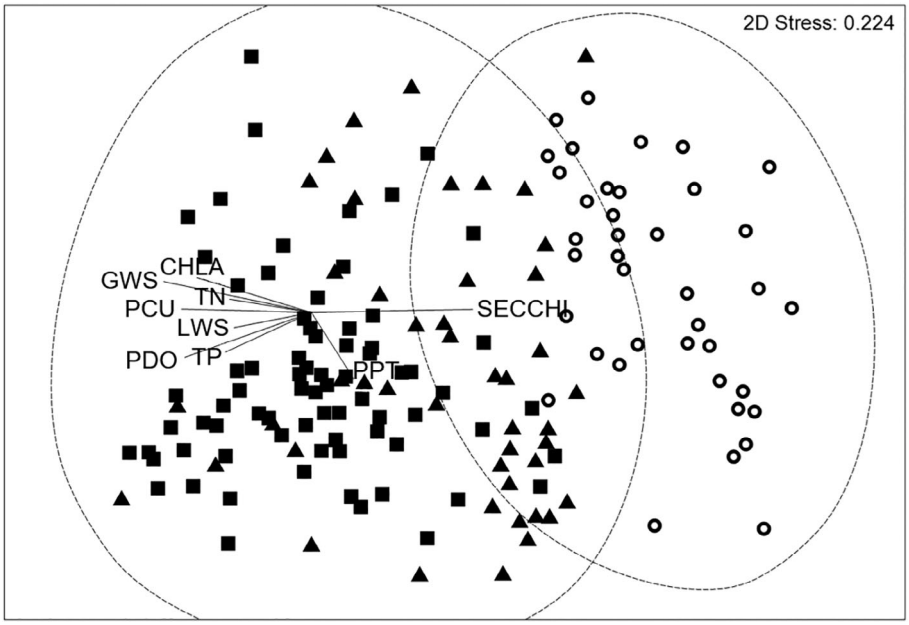

Fig. 4. Two-dimensional NMDS ordination biplot of monthly phytoplankton taxon relative biovolume. Open circles represent the clear-phytoplankton assemblage, while dark triangles and squares represent dark-phytoplankton assemblages 1 and 2, respectively. Vectors are provided for physicochemical variables explaining ≥ 30% of variance, excluding redundant variables. Vectors include Secchi disk depth (SECCHI), end-of-month total precipitation (PPT), total phosphorus (TP), Pacific Decadal Oscillation Index (PDO), lake water stage (LWS), surface water color (PCU), surface water total nitrogen (TN), groundwater stage (GWS), and surface water Chl *a* (CHLA). Dashed ellipses contain samples with > 25% compositional similarity. For specific vector strengths of all physicochemical variables see Supporting Information Table S4.

Fig. 5. Decomposed time series using a multiplicative model showing the trend component of water color (solid line) and the phytoplankton assemblage NMDS axis 1 score (dashed line) from January 2005–December 2019.

influence of wet–dry season rainfall (Supporting Information Fig. S2), resulting in the lack of relationship between seasonal phytoplankton changes and external drivers (Supporting Information Fig. S3).

Clear-water state conditions altered the phytoplankton assemblage and pattern of succession observed in the prior dark-water state through a possible twofold sequential mechanism: (1) a lowered water table reduced the magnitude of allochthonous inflows of nutrients and CDOC, likely allowing for (2) an increased role of regulation by internal nutrient loading, competition, parasitism, and predation. Without consistent seasonal pulses of allochthonous CDOC and nutrients, seasonal and interannual clear-state phytoplankton assemblages were less repeatable year-to-year. An increase in mean water residence time from 9.1 months in dark-water state to 13.5 months in the clear-water state likely contributed to the difference in the lag time in phytoplankton assemblage response, and the quicker reversion of the phytoplankton back to dark-phytoplankton assemblage dynamics also suggests a resilience engendered by repeatable seasonal pulses of external drivers (CDOC and nutrients). In the dark-water states, algal priming may have contributed to increased resilience of phytoplankton assemblages as algae-produced DOC can stimulate heterotrophic decomposition of recalcitrant carbon, increasing inorganic nutrient availability for primary producers (Guenet et al. 2010).

Lake hydrology and physicochemistry

Long-term data are imperative to the detection of climate oscillations, which can influence the physicochemistry and biology of lakes via hydrologic effects on timescales of years to decades (Harris and Baxter 1996; Winder and Schindler 2004; Gaiser et al. 2009b). While the AMO has previously been shown to control CDOC fluxes in Lake Annie (Gaiser et al. 2009b) and other Florida water bodies such as the Everglades (Regier et al. 2016), Lake Annie's hydrology (groundwater stage [GWS], lake water stage [LWS]) and water clarity were not strongly correlated with the multidecadal signal of the

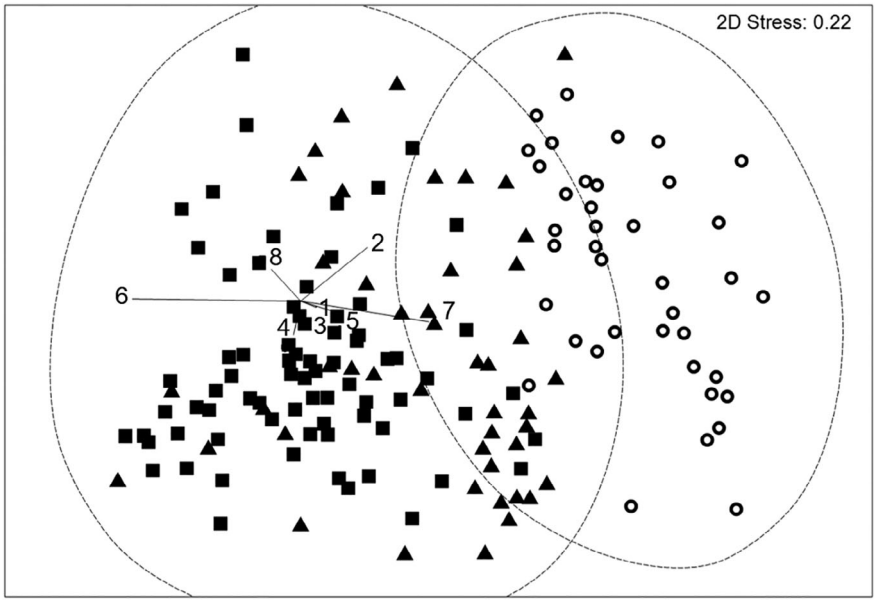

Fig. 6. Two-dimensional NMDS ordination biplot of taxon relative biovolumes with vectors indicating MBFGs). Open circles represent the clear-phytoplankton assemblage, while dark triangles and squares represent dark-phytoplankton assemblages 1 and 2, respectively. Dashed ellipses contain samples with > 25% compositional similarity. MBFGs include (1) small organisms with high surface area to volume ratio, (2) small flagellated organisms with siliceous exoskeletal structures, (3) large filaments with aerotopes, (4) medium size organisms lacking specialized traits, (5) medium to large size unicellular flagellates, (6) nonflagellated organisms with siliceous exoskeletons, (7) large mucilaginous colonies, and (8) large filaments lacking aerotopes.

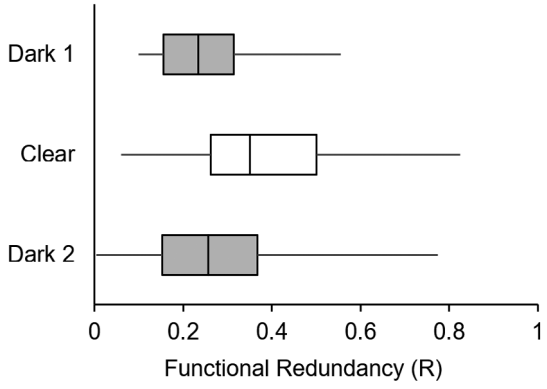

Fig. 7. Boxplots showing minimum, median, and maximum functional redundancy for dark-phytoplankton assemblage 1, clear-phytoplankton assemblage, and dark-phytoplankton assemblage 2.

AMO over the time frame of this study. The 14-yr record of this study may have been too short to detect any AMO driver, as this teleconnection tends to influence Florida rainfall on longer timescales of 65–80 yr (Enfield et al. 2001). The two transitions in water color state from 2005 to 2019 were strongly associated with phase transitions of the PDO (Fig. 2), though this relationship remains strictly correlative as the PDO switches between warm and cool phases approximately every 20–35 yr (Winder and Schindler 2004), necessitating a longer period of study to accurately describe the relationships between PDO and lake hydrology.

Across a variety of ecosystems, the net impact of a disturbance is greatly influenced by antecedent conditions (Holling 1973; Standish et al. 2014; Angeler and Allen 2016). In South Central Florida, yearly precipitation shifts associated with wet and dry seasons strongly regulate nutrient cycling within lakes (Gaiser et al. 2009a), and lakes are believed to be more resilient to acute system disturbances (e.g., storms and cold-snaps) when rainfall seasonality is interannually consistent (Kolding and Van Zwieten 2012; De Senerpont Domis et al. 2013). In Lake Annie, a 2010–2011 winter cold snap coinciding with the clear-water state prompted the coldest January holomictic conditions on record. Though thermal stability tends to decrease with increasing water clarity (Solomon et al. 2015), the winter cold-snap caused greater-than-expected thermal stability in the following summer months, negating decreased thermal-stability predicted in hypothesis H1. The absence of strong seasonal and interannual hydrologic drivers during the clear-water phase may have resulted in decreased lake resilience to this cold-snap disturbance.

The implications of hydrologic regulation of Florida lakes may be extended to other lakes throughout the world as warming temperatures and altered precipitation patterns are predicted to cause many lakes to shift from dimictic to monomictic mixing regimes (Woolway and Merchant 2019; Woolway et al. 2020). With reduced thermal regulation of lake physics also comes decreased regulation of phytoplankton succession. Cold winter conditions that act as a reset to

phytoplankton succession in dimictic lakes may become inferior to seasonal fluctuations in nutrients and CDOC which dictate succession patterns in many subtropical and tropical lakes (Lewis 1978; De Senerpont Domis et al. 2013), including Lake Annie. With greater variability in external inputs and narrower seasonal temperature fluctuations, dimictic lakes and their biota may become less resilient to disturbances and lakes that are currently monomictic may serve as important analogs for understanding these climate-driven changes (Porter et al. 1996).

Despite evidence that browning suppresses primary production in many temperate lakes (Carpenter and Pace 1997; Solomon et al. 2015; Kritzberg et al. 2020), Chl *a* concentrations in Lake Annie were higher during the dark- than clear-water state, likely due to increased external nutrient inputs. It is likely that CDOC concentrations during the dark-water state were never great enough to limit light availability (see theoretical model, Kelly et al. 2018). Though lake metabolism was not calculated during this study, prior studies of Swedish lakes have determined state shifts from net phototrophy to net heterotrophy occur around a DOC threshold of 10–11 mg L^{-1} (Jansson et al. 2000; Bergström and Karlson 2019). As Lake Annie's dark-water state DOC concentrations were on the cusp of this threshold (10.5 mg L^{-1}), concentrations of DOC may not have been high enough to stimulate phytoplankton mixotrophy, characteristic of many brown-water lakes (Wilken et al. 2017; Kritzberg et al. 2020; Senar et al. 2021). Water quality thresholds such as this may also be affected by ecological memory—where past states influence future responses of an ecosystem and its biota (Padisák 1992). For example, frequent wet-season storms may have promoted repeatable succession in dark-phytoplankton assemblages via seasonal resuspension of algal propagules from sediments, along with favorable nutrient conditions for germination (as described by Padisák 1992). Algal recruitment from the sediments could have been suppressed during the low-nutrient clear-water state, yet the quick reversion of the phytoplankton to prior dark-phytoplankton assemblage dynamics following increased nutrients and DOC further supports ecological memory of antecedent conditions (Padisák 1992). Phytoplankton may therefore help maintain dark-water state conditions or contribute to resilience via timed seasonal reoccurrence and amplification of favorable traits.

Phytoplankton assembly and function

A total of 279 taxa from 8 algae phyla were identified from Lake Annie over the course of this study (Supporting Information Table S1), many of which are unique to subtropical and low-nutrient water bodies. A notable increase in desmid richness occurred during the clear state, with nearly 100 desmid species identified. As local desmid extinctions become a widespread phenomenon (Hansen et al. 2018), low-nutrient, acidic water bodies like Lake Annie may become important refugia for these rare and sensitive taxa. Overall, phytoplankton assemblage analyses were supportive of our hypotheses, suggesting phytoplankton remain a valuable metric in the assessment of ecosystem resilience due to their acute sensitivity to environmental change (Reynolds et al. 2002).

The structural differences among dark- and clear-phytoplankton assemblages in Lake Annie were best described by MBFGs which prioritize the relationship of species phenotypic traits rather than taxonomic linkages (Kruk et al. 2010; Supporting Information Fig. S5). The largest change in assemblage between states was the unusually low abundance of diatoms (MBFG 6) in the clear-phytoplankton assemblage, comprising a mean 2% of total biovolume compared to 42% in the dark-phytoplankton assemblages. At least one other study has found prolonged low abundance of diatoms associated with a period of drought and low runoff, likely caused by altered nutrient availability or parasitism, as dissolved reactive silica (DRSi) was ample (Carey et al. 2016). In Lake Annie, DRSi depletion cannot be ruled out as the cause of the near-disappearance of diatoms because DRSi concentrations were not measured; however, it is unlikely that silica was completely depleted because there was a corresponding increase in the abundance of silica-scaled synurophytes (MBFG 2) when diatoms were sparse. Most diatoms prioritize cellular division over energy storage, so populations are rarely maintained during periods of prolonged silica depletion. In contrast, synurophytes can store physiologically active silicate in excess during periods of severe DRSi depletion, and thus their growth is only influenced by long-term exhaustion (Klaveness and Guillard 1975; Sandgren et al. 1996). If ambient DRSi concentrations were low in Lake Annie during the clear-phytoplankton assemblage, it is possible that synurophytes were able to outcompete common larger diatoms.

Smaller diatoms (e.g., *Aulacoseira tenella*) that have similar silica content to synurophytes (Klaveness and Guillard 1975) were likely underrepresented in this study as all samples were collected with a 20-μm plankton net. Though synurophytes are also in the nanoplankton size range, colonial arrangements (*Synura* spp.) and the presence of spines (*Mallomonas* spp.) may have prevented their underestimation in net tows. Smaller species made up a larger proportion of the clear-phytoplankton assemblage (Supporting Information Fig. S6) including the desmid *Cosmarium pseudotaxichondrum* v. *scotti* and small colonial cyanobacteria such as *Merismopedia* spp. The greater surface area to volume ratio of small cells is associated with increased uptake efficiency of limiting nutrients, and consequently may make them superior competitors for phosphorus during periods of decreased nutrient loading due to drought (Harris and Baxter 1996) or a return to oligotrophic conditions (Litchman et al. 2007; Anneville et al. 2018). Small taxa can therefore promote internal feedbacks where high nutrient uptake affinity aids in the maintenance of low-nutrient conditions (Litchman et al. 2007). Increased abundances of small diatoms such as *Discostella stelligera* have also been recorded in warming lakes where winter mixing depths

are decreased (Saros et al. 2016), but because there were no strong differences in stratification length or thermocline depth during the stratified period in Lake Annie between dark and clear states, assemblage shifts were likely driven by hydrologically regulated changes in light and nutrient availability, and less so by temperature (De Senerpont Domis et al. 2013).

In Lake Annie, dinoflagellates showed no strong preference for clear- or dark-water states, though mixotrophic *Dinobryon* species were more common in clear-phytoplankton assemblages suggesting carbon deficiencies were the primary driver of *Dinobryon* presence rather than light scarcity. Although more commonly reported in brown-water lakes (Jones 2001; Wilken et al. 2017; Senar et al. 2021), mixotrophic dinoflagellates and chrysophytes are also common in lakes with persistent clear-water states (Lydén and Grahn 1985; Deininger et al. 2017), where nutrient supplies are suppressed but bacteria still serve as a valuable carbon source (Bird and Kalff 1987; Findlay et al. 2001). In the clear-phytoplankton assemblages when diatoms were in very low abundance, succession was less repeatable across years, but always began with a late winter or early spring peak of Ochrophytes, usually *Synura petersenii* (Supporting Information Fig. S5b). While spring silicoflagellate blooms are common in oligotrophic lakes (Sommer et al. 1986), the absence of any apparent diatom seasonality is unusual and may have contributed to the lack of repeatability of these trends.

The near disappearance of diatoms in the clear-water state may have also contributed to greater evenness among remaining functional groups, leading to greater-than-expected mean functional redundancy in the clear-water state. While the Ricotta et al. (2016) method has been widely used to assess functional redundancy across a variety of flora and fauna, we did not find any explicit use of this method for phytoplankton assemblages. Typically, absolute abundance data are used in functional redundancy analyses of plant and animal communities but because phytoplankton cell sizes vary considerably, functional units (e.g., colonies, filaments, or unicells) rather than cells may be a more appropriate representation of a given species' contribution to a functional group (see Kruk et al. 2017). This corrects for an overestimation of the functional contribution of small cells which are more heavily weighted in an absolute abundance analysis. Due to ease of use and interpretation, we are hopeful the Ricotta et al. (2016) method can be applied in future works assessing lake ecosystem resilience with the suggested modifications toward phytoplankton communities.

Conclusions

In temperate lakes, browning generally causes disruptions to archetypal phytoplankton successional dynamics (Wilken et al. 2017; Kritzberg et al. 2020) yet in Lake Annie, seasonal phytoplankton dynamics depend on the pulses of CDOC and nutrients driven by seasonal wet–dry hydrology to maintain assemblage stability. Duration and intensity of hydrologic alterations may result in short-term (Harris and Baxter 1996; Carey et al. 2016) or long-term changes in phytoplankton assemblage (Kamenir et al. 2004), therefore studying lakes with oscillating periods of clear- and dark-water states provides a unique insight into phytoplankton responses—and possibly feedbacks—to cyclical regime shifts.

Over the course of this study (October 2005–December 2019), Lake Annie fluctuated between dark- and clear-water states, largely driven by groundwater levels. When GWS was high (dark-water states), the influence of wet–dry season hydrology was strong and phytoplankton succession was more repeatable year to year with patterns similar to those described in many temperate dimictic lakes (Sommer et al. 1986). The strong and predictable seasonality of abiotic changes (CDOC and nutrients) during dark-water states facilitated the rapid recovery of a dark-water phytoplankton assemblage exhibiting anticipated succession patterns after transitioning from a prior clear-water assemblage. When GWS was low (clear-water state), the lack of strong external seasonal pulses of CDOC and nutrients reduced predictable succession in the clear-phytoplankton assemblage, which was likely more highly regulated by competition (e.g., small taxa with better nutrient uptake efficiency) and possibly predation.

By metrics of functional redundancy and multivariate analyses, we believe stronger, seasonally consistent hydrologic controls promoted greater ecosystem resilience in Lake Annie during dark-water states. In browning lakes, assessment of phytoplankton assembly could serve as an important tool in detecting the direct and indirect consequences of DOC shifts on lake resilience. In addition, as rainfall variability continues to increase under a warming climate (Pendergrass et al. 2017), subtropical lakes that are already strongly influenced by regional hydrology could serve as important analogs for the potential responses of dimictic lakes as they transition to monomictic thermal regimes (Porter et al. 1996; Woolway and Merchant 2019; Woolway et al. 2020).

References

Angeler, D. G., and C. R. Allen. 2016. Quantifying resilience. J. Appl. Ecol. **53**: 617–624. doi:10.1111/1365-2664.12649

Anneville, O., G. Dur, F. Rimet, and S. Souissi. 2018. Plasticity in phytoplankton annual periodicity: An adaptation to long-term environmental changes. Hydrobiologia **824**: 121–141. doi:10.1007/s10750-017-3412-z

Battoe, L. 1987. Report of limnological research on Lake Annie. Postdoctoral research report, Archbold Biological Station.

Bergström, A., and J. Karlson. 2019. Light and nutrients control phytoplankton biomass responses to global change in northern lakes. Global Change Biol. **25**: 2021–2029. doi:10.1111/gcb.14623

Bertilsson, S., and L. J. Tranvik. 2000. Photochemical transformation of dissolved organic matter in lakes. Limnol. Oceanogr. **45**: 753–762. doi:10.4319/lo.2000.45.4.0753

Bird, D. F., and J. Kalff. 1987. Algal phagotrophy: Regulating factors and importance relative to photosynthesis in *Dinobryon* (Chrysophyceae). Limnol. Oceanogr. **32**: 277–284. doi:10.4319/lo.1987.32.2.0277

Bishop, E. W. 1956. Geology and ground-water resources of Highlands County, Florida. Report of Investigations #15, Florida Geological Survey, DOI: 10.1113/jphysiol.1956.sp005664.

Canfield, D. E., Jr., S. B. Linda, and L. M. Hodgson. 1984. Relations between color and some limnological characteristics of Florida lakes. J. Am. Water Resour. Assoc. **20**: 323–329. doi:10.1111/j.1752-1688.1984.tb04711.x

Carey, C. C., P. C. Hanson, R. C. Lathrop, and A. L. St. Amand. 2016. Using wavelet analyses to examine variability in phytoplankton seasonal succession and annual periodicity. J. Plankton Res. **38**: 27–40. doi:10.1093/plankt/fbv116

Carpenter, S. R., and M. L. Pace. 1997. Dystrophy and eutrophy in lake ecosystems: Implications of fluctuating inputs. Oikos **78**: 3–14. doi:10.2307/3545794

Chow G. C. 1960. Tests of Equality Between Sets of Coefficients in Two Linear Regressions. Econometrica **28**: 591. doi:10.2307/1910133

Clarke, K. R., and R. N. Gorley. 2015. Getting started with PRIMER v7. PRIMER-E Ltd.

Curtis, S. 2008. The Atlantic multidecadal oscillation and extreme daily precipitation over the US and Mexico during the hurricane season. Climate Dynam. **30**: 343–351. doi:10.1007/s00382-007-0295-0

Deininger, A., C. L. Faithfull, and A.-K. Bergström. 2017. Phytoplankton response to whole lake inorganic N fertilization along a gradient in dissolved organic carbon. Ecology **98**: 982–994. doi:10.1002/ecy.1758

De Senerpont Domis, L. N., and others. 2013. Phytoplankton dynamics under different climatic conditions in space and time. Freshw. Biol. **58**: 463–482. doi:10.1111/fwb.12053

Enfield, D. B., A. M. Mestas-Nuñez, and P. J. Trimble. 2001. The Atlantic multidecadal oscillation and its relation to rainfall and river flows in the continental U.S. Geophys. Res. Lett. **28**: 2077–2080. doi:10.1029/2000GL012745

Findlay, D. L., S. E. M. Kasian, M. P. Stainton, K. Beaty, and M. Lyng. 2001. Climatic influences on algal populations of boreal forest lakes in the Experimental Lakes area. Limnol. Oceanogr. **46**: 1784–1793. doi:10.4319/lo.2001.46.7.1784

Florida LAKEWATCH. 2020. Florida LAKEWATCH water chemistry field sampling and laboratory protocols. Fisheries and Aquatic Sciences, School of Forest Resources and Conservation/IFAS, Univ. of Florida.

Gaiser, E. E., N. D. Deyrup, R. W. Bachmann, L. E. Battoe, and H. M. Swain. 2009*a*. Effects of climate variability on transparency and thermal structure in subtropical, monomictic Lake Annie, Florida. Fund. Appl. Limnol **175**: 217–230. doi:10.1127/1863-9135/2009/0175-0217

Gaiser, E. E., N. D. Deyrup, R. W. Bachmann, L. E. Battoe, and H. M. Swain. 2009*b*. Multidecadal climate oscillations detected in a transparency record from a subtropical Florida lake. Limnol. Oceanogr. **54**: 2228–2232. doi:10.4319/lo.2009.54.6.2228

Guenet, B., M. Danger, L. Abbadie, and G. Lacroix. 2010. Priming effect: bridging the gap between terrestrial and aquatic ecology. Ecology **91**: 2850–2861. doi:10.1890/09-1968.1

Hammer, Ø., D. A. T. Harper, and P. D. Ryan. 2001. PAST: Paleontological statistics software package for education and data analysis. Palaeontol. Electron. **4**: 9.

Hansen, G., J. Stastny, Ø. Moestrup, and N. Lundholm. 2018. Diversity and conservation of desmids in Bornholm, Denmark—Revisiting after 130 years. Nord. J. Bot. **36**: e01994. doi:10.1111/njb.01994

Harris, G. P., and G. Baxter. 1996. Interannual variability in phytoplankton biomass and species composition in a subtropical reservoir. Freshw. Biol. **35**: 545–560. doi:10.1111/j.1365-2427.1996.tb01768.x

Holling, C. S. 1973. Resilience and stability of ecological systems. Annu. Rev. Ecol. Evol. Syst. **4**: 1–23. doi:10.1146/annurev.es.04.110173.000245

Jansson, M., A. Bergström, P. Blomqvist, and S. Drakare. 2000. Allochthonous organic carbon and phytoplankton/bacterioplankton production relationships in lakes. Ecology **81**: 3250–3255 doi:10.1890/0012-9658(2000)081[3250:AOCAPB]2.0.CO;2.

Jones, R. I. 2001. Mixotrophy in planktonic protists: An overview. Freshw. Biol. **45**: 219–226. doi:10.1046/j.1365-2427.2000.00672.x

Kamenir, Y., Z. Dubinsky, and T. Zohary. 2004. Phytoplankton size structure stability in a meso-eutrophic subtropical lake. Hydrobiologia **520**: 89–104. doi:10.1023/B:HYDR.0000027729.53348.c7

Kelly, P. T., C. T. Solomon, J. A. Zwart, and S. E. Jones. 2018. A framework for understanding variation in pelagic gross primary production of lake ecosystems. Ecosystems **21**: 1364–1376. doi:10.1007/s10021-018-0226-4

Klaveness, D., and R. R. L. Guillard. 1975. The requirement for silicon in *Synura petersenii* (Chrysophyceae). J. Phycol. **11**: 349–355. doi:10.1111/j.1529-8817.1975.tb02795.x

Kolding, J., and P. A. M. van Zwieten. 2012. Relative lake level fluctuations and their influence on productivity and resilience in tropical lakes and reservoirs. Fish. Res. **115-116**: 99–109. doi:10.1016/j.fishres.2011.11.008

Kritzberg, E. S., and others. 2020. Browning of freshwaters: Consequences to ecosystem services, underlying drivers, and potential mitigation measures. Ambio **49**: 375–390. doi:10.1007/s13280-019-01227-5

Kruk, C., and others. 2017. Functional redundancy increases towards the tropics in lake phytoplankton. J. Plankton Res. **39**: 518–530. doi:10.1093/plankt/fbw083

Kruk, C., V. L. M. Huszar, E. T. H. M. Peeters, S. Bonilla, L. Costa, M. Lürling, C. Reynolds, and M. Scheffer. 2010. A

morphological classification capturing functional variation in phytoplankton. Freshw. Biol. **55**: 614–627. doi:10.1111/j.1365-2427.2009.02298.x

Leles, S. G., L. Polimene, J. Bruggeman, J. Blackford, S. Ciavatta, A. Mitra, and K. J. Flynn. 2018. Modelling mixotrophic functional diversity and implications for ecosystem function. J. Plankton Res. **40**: 627–642. doi:10.1093/plankt/fby044

Lewis, W. M. 1978. Dynamics and succession of the phytoplankton in a tropical lake: Lake Lanao, Philippines. J. Ecol. **66**: 849–880. doi:10.2307/2259300

Litchman, E., C. A. Klausmeier, O. M. Schofield, and P. G. Falkowski. 2007. The role of functional traits and trade-offs in structuring phytoplankton communities: Scaling from cellular to ecosystem level. Ecol. Lett. **10**: 1170–1181. doi:10.1111/j.1461-0248.2007.01117.x

Lydén, A., and O. Grahn. 1985. Phytoplankton species composition, biomass, and production in Lake Gårdsjön—An acidified Clearwater lake in SW Sweden. Ecol. Bull. **37**: 195–202.

Moses, C. S., W. T. Anderson, C. Saunders, and F. Sklar. 2013. Regional climate gradients in precipitation and temperature in response to climate teleconnections in the Greater Everglades ecosystem of South Florida. J. Paleolimnol. **49**: 5–14. doi:10.1007/s10933-012-9635-0

Olson, C. R., C. T. Solomon, and S. E. Jones. 2020. Shifting limitation of primary production: Experimental support for a new model in lake ecosystems. Ecol. Lett. **23**: 1800–1808. doi:10.1111/ele.13606

Pace, M. L., and J. J. Cole. 2002. Synchronous variation of dissolved organic carbon and color in lakes. Limnol. Oceanogr. **47**: 333–342. doi:10.4319/lo.2002.47.2.0333

Padisák, J. 1992. Seasonal succession of phytoplankton in a large shallow lake (Balaton, Hungary)—A dynamic approach to ecological memory, its possible role and mechanisms. J. Ecol. **80**: 217–230. doi:10.2307/2261008

Pendergrass, A. G., R. Knutti, F. Lehner, C. Deser, and B. M. Sanderson. 2017. Precipitation variability increases in a warmer climate. Sci. Rep. **7**: 17966. doi:10.1038/s41598-017-17966-y

Porter, K. G., P. A. Saunders, K. A. Haberyan, A. E. Macubbin, T. R. Jacobsen, and R. E. Hodson. 1996. Annual cycle of autotrophic and heterotrophic production in a small, monomictic Piedmont lake (Lake Oglethorpe): Analog for the effects of climate warming on dimictic lakes. Limnol. Oceanogr. **41**: 1041–1051. doi:10.4319/lo.1996.41.5.1041

R Core Team. 2019. R: A language and environment for statistical computing. R Foundation for Statistical Computing, . https://www.R-project.org/.

Regier, P., H. Briceño, and R. Jaffé. 2016. Long-term environmental drivers of DOC fluxes: Linkages between management, hydrology and climate in a subtropical coastal estuary. Estuarine, Coastal and Shelf Science **182**: 112–122. doi:10.1016/j.ecss.2016.09.017

Reynolds, C. S., V. Huszar, C. Kruk, L. Naselli-Flores, and S. Melo. 2002. Towards a functional classification of the freshwater phytoplankton. Journal of Plankton Research **24**: 417–428. doi:10.1093/plankt/24.5.417

Ricotta, C., F. de Bello, M. Moretti, M. Caccianiga, B. E. L. Cerabolini, and S. Pavoine. 2016. Measuring the functional redundancy of biological communities: A quantitative guide. Methods Ecol. Evol. **7**: 1386–1395. doi:10.1111/2041-210X.12604

Sandgren, C. D., S. A. Hall, and S. B. Barlow. 1996. Siliceous scale production in chrysophyte and synurophyte algae. 1. Effects of silica-limited growth on cell silica content, scale morphology, and the construction of the scale layer of *Synura petersenii*. J. Phycol. **32**: 675–692. doi:10.1111/j.0022-3646.1996.00675.x

Saros, J. E., R. M. Northington, D. S. Anderson, and N. J. Anderson. 2016. A whole-lake experiment confirms a small centric diatom species as an indicator of changing lake thermal structure. Limnol. Oceanogr. Lett. **1**: 27–35. doi:10.1002/lol2.10024

Senar, O. E., I. F. Creed, and C. G. Trick. 2021. Lake browning may fuel phytoplankton biomass and trigger shifts in phytoplankton communities in temperate lakes. Aquat. Sci. **83**: 1–15. doi:10.1007/s00027-021-00780-0

Solomon, C. T., and others. 2015. Ecosystem consequences of changing inputs of terrestrial dissolved organic matter to lakes: Current knowledge and future challenges. Ecosystems **18**: 376–389. doi:10.1007/s10021-015-9848-y

Sommer, U., Z. M. Gliwicz, W. Lampert, and A. Duncan. 1986. The PEG-model of seasonal succession of planktonic events in fresh waters. Arch. Hydrobiol. **106**: 433–471.

Standish, R. J., and others. 2014. Resilience in ecology: Abstraction, distraction, or where the action is? Biol. Conserv. **177**: 43–51. doi:10.1016/j.biocon.2014.06.008

Stockwell, J. D., and others. 2020. Storm impacts on phytoplankton community dynamics in lakes. Global Change Biol. **26**: 2756–2784. doi:10.1111/gcb.15033

Wilken, S., M. Soares, P. Urrutia-Cordero, J. Ratcovich, M. K. Ekvall, E. Van Donk, and L. A. Hansson. 2017. Primary producers or consumers? Increasing phytoplankton bacterivory along a gradient of lake warming and browning. Limnol. Oceanogr. **63**: S142–S155. doi:10.1002/lno.10728

Winder, M., and D. E. Schindler. 2004. Climate effects on the phenology of lake processes. Global Change Biol. **10**: 1844–1856. doi:10.1111/j.1365-2486.2004.00849.x

Winslow, L., Read, J., Woolway, R., Brentrup, J., Leach, T., Zwart, J., Albers, S., and D. Collinge. 2019. rLakeAnalyzer: Lake physics tools. R package version 1.11.4.1. https://CRAN.R-project.org/package=rLakeAnalyzer, DOI: 10.3389/fpsyg.2019.02043

Woolway, R. I., and C. J. Merchant. 2019. Worldwide alteration of lake mixing regimes in response to climate change. Nat. Geosci. **12**: 271–276. doi:10.1038/s41561-019-0322-x

Woolway, R. I., B. M. Kraemer, J. D. Lenters, C. J. Merchant, C. M. O'Reilly, and S. Sharma. 2020. Global lake responses to climate change. Nat. Rev. Earth Environ **1**: 388–403. doi: 10.1038/s43017-020-0067-5

Acknowledgments

The authors would like to acknowledge the following personnel and funding agencies: Dr. Rudolf Jaffé, Dr. John Kominoski, Dr. Sparkle Malone, Franco Tobias, Ileana Corsi, Kristen Dominguez, Archbold staff Nancy Deyrup and Kevin Main, Florida LAKEWATCH and the Florida Coastal Everglades Long-Term Ecological Research program under Cooperative Agreement #DEB-1832229. This paper was developed in collaboration with the Global Lake Ecological Observatory Network and the long-time support of Archbold Biological Station. EEG is supported by the George M. Barley Jr. Endowment. This is contribution number 1372 from the Institute of Environment at Florida International University.

Conflict of Interest

None declared.

Submitted 16 February 2021
Revised 23 August 2021
Accepted 12 December 2021

Associate editor: Michael - GUEST EDITOR L Pace